Analysis of Thermo-Mechanical Stresses and Strains for a Novel Design of Insulating Glass Flat-Plate Collector

Thorsten Summ[1], Brian Sturm[1], Christian Scherer[2], Christoph Trinkl[1], and Wilfried Zörner[1]

[1] Institute of new Energy Systems, Technische Hochschule Ingolstadt, Ingolstadt (Germany)

[2] H.B. Fuller Deutschland GmbH | Kömmerling Chemische Fabrik GmbH, Pirmasens (Germany)

Abstract

Insulating glass flat-plate collectors have been investigated more intensively during the last decade as this innovative design approach promises to lower heat generation cost for solar thermal applications. The latest investigations in that field indicate that high temperatures and mechanical stresses may affect durability and stability of the collector sealings that are required for an efficient operation of the solar thermal module. A novel design was proposed recently that has not yet been studied regarding its thermo-mechanical loads, stresses, and strains. The objective of this study was to determine typical load profiles for such collectors and – through finite element analysis – determine stresses and strains on the collector sealings. An answer should be given as to whether the novel design improves the thermo-mechanical resilience of the collector and whether the chosen design can withstand typical load conditions for solar district heating. The results show that stagnation is likely to cause gas leakages but unlikely to cause mechanical failure of the collector. Furthermore, it was shown that thermo-mechanical loads during normal operation are uncritical, which is why the novel insulating glass flat-plate collector design is considered superior over the previous. Although a lifetime of 20 to 25 years is very likely to be achieved for the collector, we strongly suggest avoiding stagnation for the collector to avoid gas leakage and resulting decrease in thermal performance.

Keywords: thermo-mechanical analysis, stress, strain, finite element analysis, insulating glass, solar thermal, flat-plate collector, durability

1. Introduction

One recent approach to obtain more cost-effective solar thermal components and systems is to establish the insulating glass flat-plate collector (IGFPC). This novel collector design features low production and system cost while offering comparable thermal performance as conventional flat-plate collectors. This makes it particularly promising for solar district heating (SDH) applications. Since 2014, investigations on IGFPCs were carried out from several research institutions and are still ongoing. So far, their work mainly focused on thermal performance and thermal losses, thermomechanical stresses, durability, production techniques and estimated collector costs.

Simulation studies (Leibbrandt and Schabbach, 2015; Riess et al., 2016), indoor (Giovannetti et al., 2014; Riess, 2017) and outdoor (Giovannetti and Kirchner, 2015; Summ et al., 2023) performance tests showed that the thermal efficiency of these modules is comparable to conventional flat-plate collectors. This is mainly due to the inert gas argon which can be filled inside the enclosed cavity of the collector. This gas surrounds the absorber, has lower thermal conductivities than air, and hence reduces the convective losses of the collector.

However, durability analyses (Giovannetti and Kirchner, 2015) have shown that the insulating glass module sealings experience high thermal and mechanical loads which represent a challenge to maintain collector durability over a longer period of time. Throughout the years, several designs have been developed that impose different thermo-mechanical loads on the sealings. Whereas a pure glass collector design (Leibbrandt and Schabbach, 2015) suffers from low thermal conductivities in the absorbing element, a design setup where the absorber is bonded to the glass (Riess et al., 2015) leads to large absorber deflections causing damage to the coating or significant reductions in thermal performance (Riess et al., 2014; Riess, 2017).

Further experimental research suggests that the argon concentration significantly affects the thermal performance of the modules once the argon concentration inside the collector drops below 50 % (Summ et al., 2023). As the argon gas cost is negligible compared to the overall production cost, the target for collector producers is to achieve the highest possible concentration during production and maintain a value above 50 % during the collector lifetime of 20-25 years. This will lead to IGFPCs with both long-term durability and high performance, but also implies that the

10.18086/swc.2023.04.14 Available at http://proceedings.ises.org

sealings must withstand all imposed thermomechanical stresses and strains.

The most recently proposed collector design (Summ et al., 2020) uses a roll-bond absorber that is placed between the glass front and back pane as seen in Fig. 1. This IGFPC design proved to be the so far most efficient one (Summ et al., 2023). The inlet and outlet connectors were chosen to be fed through the rear glass to reduce the thermo-mechanical loads on the sealings. First lab tests on small scale samples (Summ et al., 2021) have indicated that the temperature loads are within an acceptable range for the collector operation.

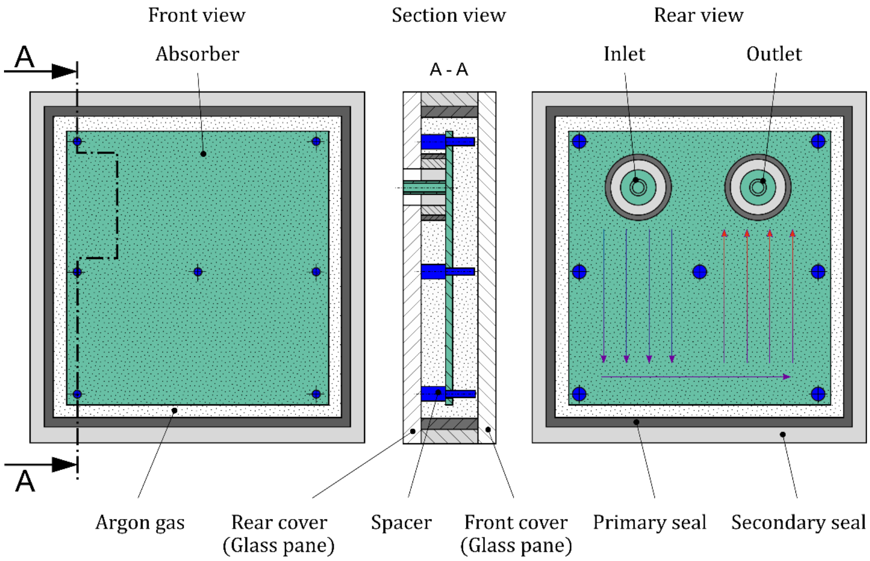

Fig. 1: Simplified sketch of the chosen insulating glass flat-plate collector design.

However, the mechanical loads and thermally induced stresses have not yet been investigated for this collector setup. The most relevant part of the collector sealing is at the inlet and outlet connectors, where the absorber is in direct contact with the sealing material. No evidence is provided whether this design improves the thermo-mechanical resilience of the collector and in that way contributes to an improvement for durability of IGFPCs. The aim of this research is to close this gap by conducting thermo-mechanical simulations and calculate the stresses and strains on the sealing material. The resulting novel outcomes of the presented study are:

- Typical operational states and resulting load conditions for IGFPCs,
- Stresses and Strains of IGFPC sealings for the so-far most efficient design.

2. Methodology

For this study, a three-stage methodological approach was chosen consisting of load analysis, thermo-mechanical finite element simulation and the analysis of stresses and strains from the simulation studies. An overview of the required inputs, methods and outcomes is given in Fig. 2. Weather data was used to determine the environmental conditions which apply to the collector for a selected site. Then, both numerical and experimental data regarding the solar thermal system behavior were taken to derive the external thermal and mechanical loads. From full-year datasets, a load profile on the collector sealings was computed using the finite element model. The results were used to compute the stresses and strains for the critical collector component – the sealings at the inlet and outlet connector.

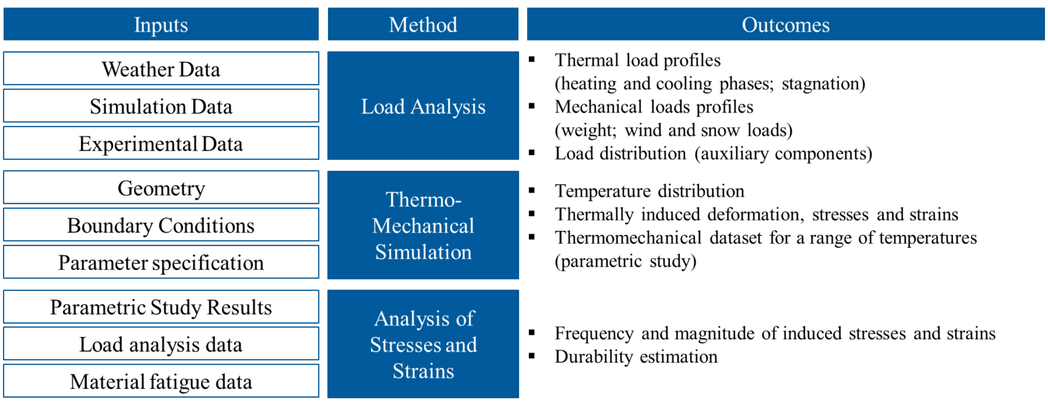

Fig. 2: Inputs, methods and outcomes chosen for this study.

2.1 Load Analysis

The loads that act on the solar thermal collectors is composed of thermal, mechanical, and thermo-mechanical loads. Thermal loads are mainly a result from the collector operation but can be distinguished into “normal” operation and the case of stagnation (e.g. when pumps fail and no heat can be dissipated from the collectors). The mechanical loads on the collector consist of its own weight, wind loads, and snow loads.

The collectors were designed for solar district heating application and for this, wind and snow load categories according to DIN EN 1991-1-3 (Deutsches Institut für Normung, 2023) and DIN EN 1991-1-4 (Deutsches Institut für Normung, 2010) were considered to define the requirements on mechanical strength. For wind load, category 4 was selected and for snow, category 3 was chosen. The sealings at the edges of the collectors correspond to the same as for insulating glass units. These were designed and validated over decades from the insulating glass industry to withstand wind/snow loads. The uncertain part for IGFPCs are therefore the sealings at the inlet and outlet connector.

However, the position of the collector inlets and outlets is near to the edges which leads to low bending loads on their sealings. Furthermore, the normal forces due to wind/snow are intercepted via the spacer elements (c.f. Fig. 1, blue parts) at the front and transferred towards the back glass pane. Therefore, wind and snow loads were considered as negligible for the inlet and outlet connector sealings.

The remaining loads of relevance for the collector sealings represent temperature loads and thermo-mechanical loads. Temperature loads on the edge sealings of the collector are moderate compared to the loads at the inlet and outlet connector. For the latter, the absorber is in direct contact with the sealing leading to the maximum temperatures at this location. Thermally induced stresses on the sealings are also significantly higher there (Riess et al., 2014). It is therefore crucial to know the collector temperature during the operation of the system.

A real solar thermal reference system was chosen for the load analysis to obtain realistic assumptions regarding the operating conditions of IGFPCs. The system is a local district heating plant in Upper Franconia, Germany characterized by a combination of 5 biomass boilers, solar thermal flat-plate collectors, and a combined heat and power generator and a gas boiler. The grid is operated with a flow temperature of 80 °C and a return temperature of 55 °C. Fig. 3 shows the schematic diagram of the system.

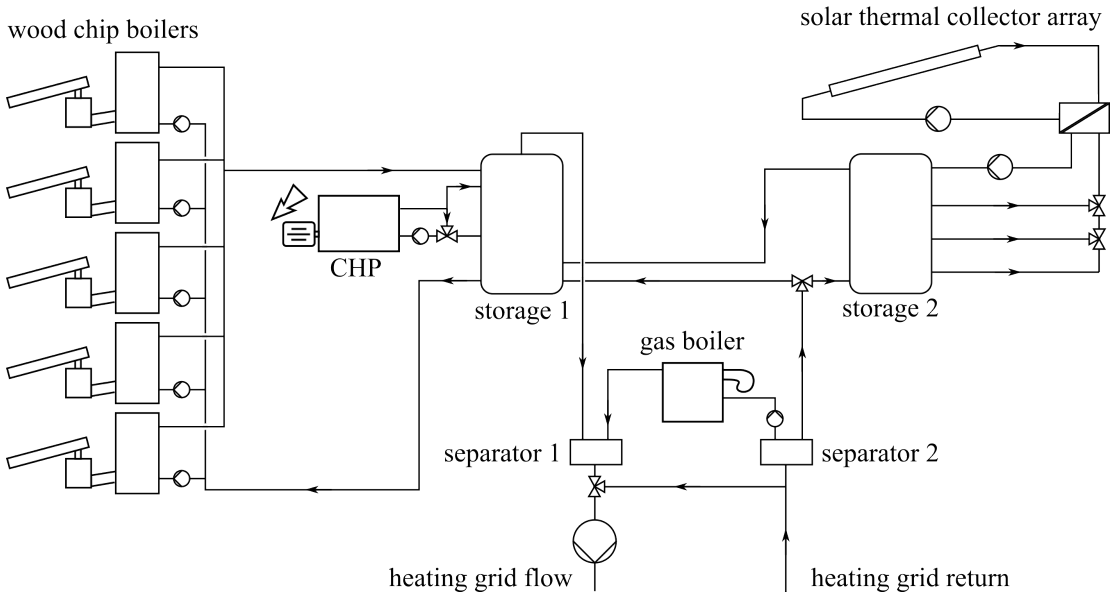

Fig. 3: Schematic diagram of the district heating system.

The base load heat generators for the district heating supply are 5 wood chip boilers with 155 kW each. They are connected to a central buffer storage 1 with a size of 20 m³. The combined heat and power system with 50 kW_{el} and 80 kW_{th} is controlled according to feed-in availabilities for the electrical grid and also connected to the buffer storage 1. The gas boiler with 450 kW is used for peak load operation. It is connected via two separators and can feed directly into the grid. The solar thermal system with 190 kW is integrated into the district heating system via a solar buffer storage 2 with a size of 20 m³. Both storages are connected in series and storage 2 can be bypassed using a 3-way-valve at the return of the heating grid. In this way, solar gains can be stored independently from the operation and temperature levels from the grid.

For this study, the solar thermal system was analyzed to obtain typical operating temperatures that will be relevant for the IGFPC operation in a district heating system. Since the higher outlet temperature is more relevant/critical for the sealing durability than the inlet temperature, the measured outlet temperature of the collector array was taken as a reference for the loads. The results of this analysis are presented in section 3.1.

2.2 Thermo-Mechanical Simulation

To compute the temperature distribution of the collector components and their induced mechanical reaction, a finite element model was created using the software ANSYS Mechanical 2022 R2 (ANSYS, Inc., 2022). Fig. 4 shows the 3D model used for the simulation. The assembly consists of 5 main components. As the collector is symmetric along its vertical principal axis, symmetry conditions were applied and the geometry was cut in half. Furthermore, the lower part of the collector – in higher distance from the inlet and outlet connectors – are not of interest and were cut off. Hence, a quarter of the collector geometry was sufficient to analyze.

The absorber of the IGFPCs described in section 1 consists of three separate sheets that are connected with each other. After applying symmetry, just an outer (1) and inner (2) sheet are left. Both are connected by an intermediate piece (5) that also contains the outlet connector geometry. This piece connects the absorber with the two sealings and the surrounding rear glass pane (4). As shown in Fig. 1, the two sealings are divided into primary and secondary sealing. Being connected to the back pane, the primary sealing provides gas-tightness, and the secondary sealing provides mechanical strength. The absorber thus sealed is protected from external environmental influences, such as rain or dust, and achieves a high degree of stability. The spacers (3), which connect the absorber with the glass pane, prevent relative motion in normal direction during thermal expansion and mechanical loads. The spacers are firmly connected to the individual absorbers and can move relative to the glass pane surface. This allows the absorber and spacers to expand when temperature increases/decreases.

For discretization of the model, a finite element mesh was created using a global mesh size of 1.5 mm and a spherical refinement region (diameter of 160 mm) with a local mesh size of 1 mm. The glass was the only component with a larger mesh size of 7 mm, but also refined as shown in Fig. 5. Tetrahedron elements with a cell node count of 847,368 and element count of 3,230,313 were used for the analysis.

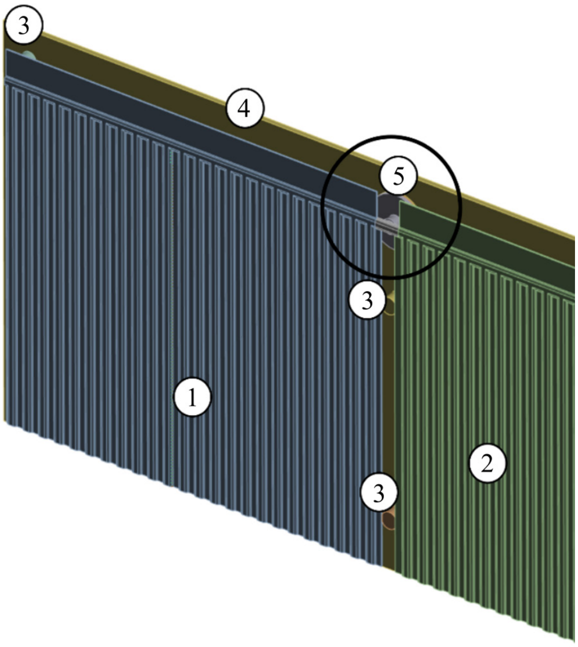

Fig. 4: Geometry of the IGFPC. The circle indicated the refinement region used for mesh generation.

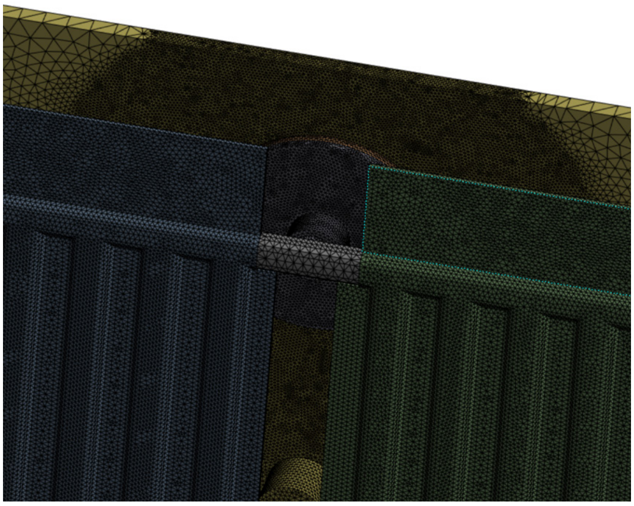

Fig. 5: Meshed geometry of the IGFPC. The refinement surrounding the outlet connector is shown.

The element size around the outlet connector is shown as a magnified view in Fig. 6. The mesh transition between multiple components was selected in such a way, that a conform mesh was generated. This enhances the computation quality, particularly in the regions where high temperature and deformation gradients are expected such as the contact area between outlet connector and primary/secondary sealing. Fig. 7 shows the distribution of element quality and the number of elements with a certain quality level in a histogram. The average element quality was 82 % and exist in the refinement area surrounding the outlet connector.

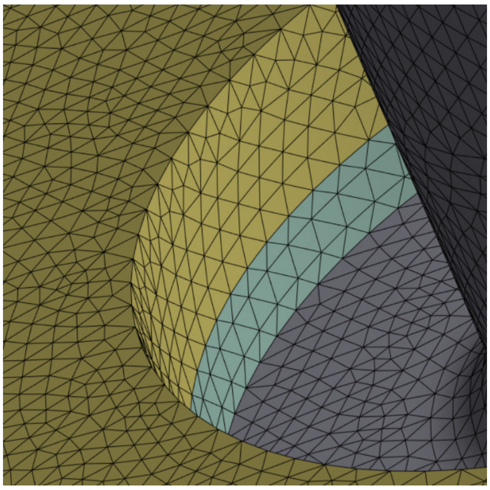

Fig. 6: Meshed geometry around the outlet connector. The transition between multiple components shows that a conform mesh was generated.

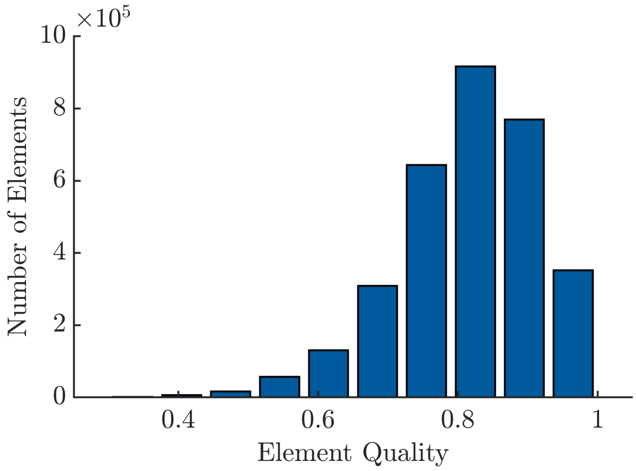

Fig. 7: Element quality histogram. The average element quality was 82 %, which corresponds to the quality range which the most elements had.

As the material properties for the sealing materials are non-linear, the analysis was a non-linear thermo-mechanical simulation. In the case of polyisobutylene, the material exhibits nonlinear behavior due to its viscoelastic properties. Under load, polyisobutylene deforms both elastically and plastically. This means that there is some elastic recovery after unloading, but there is also permanent plastic deformation. This complex behavior results in a nonlinear stress-strain relation. Silicone rubber is considered an ideally elastic (hyperelastic) material that can be described by so-called Mooney-Rivlin parameters. The non-linear material had to be treated confidentially and therefore cannot be disclosed in this paper. The remaining materials were considered to be linearelastic and therefore can be purely described by Young's modulus and Poisson's ratio. Tab. 1 shows the selected material properties for the simulation study.

Tab. 1: Selected material properties for the thermo-mechanical simulation analysis.

Component	**Material**	**Density** in kg/m³	**Young's modulus** in MPa	**Poisson's Ratio** -	**Thermal expansion** 1/K	**Heat conductivity** in W/(mK)
Absorber	EN AW 1050A	2700	70000	0.30	2.35 E-05	215
Connector	EN AW 6060	2700	70000	0.32	2.34 E-05	210
Glass pane	Float glass	2500	70000	0.23	8.50 E-06	0.76
Primary Seal	Polyisobutylene	1220	N/A	0.50	4.00 E-05	0.76
Secondary Seal	Silicone rubber	1370	N/A	0.50	27.5 E-05	0.18
Spacer	Polytetrafluoroethylene	2180	700	0.40	12.5 E-05	0.25

For the simulation, the following assumptions and simplifications were considered:

- Gravitational acceleration does not act on the components;
- No fluid domains are present;
- The absorber has a homogeneous and constant temperature;
- There is no convective loss from absorber or connector to the inter-pane gas cavity;
- The sealings at the collector edges are not considered;
- The front glass is not considered, but the rear glass with convective losses towards the ambient air.

The load profiles and characteristics obtained from the analysis described in section 2.1 were applied as temperature boundary conditions for the thermo-mechanical simulation. To reduce complexity of the model, the inter-pane cavity containing the argon gas was not included to the model. We assumed that the gas temperature inside the collector is equal to the absorber temperature, although for a real case, the gas will show significantly lower temperatures. A steady-state analysis was chosen for the analysis computing the equilibrium states for different temperature levels.

The boundary conditions that were chosen for the analysis are listed in Tab. 2. All contacts affecting the sealings were chosen as type 'bonded' because the special primary and secondary sealings (HelioSeal and HelioBond) not only adhere to the surface of the adjacent materials but also establish a chemical bond between them. The contact between absorber and connector is a soldered junction and therefore bonded as well. A frictionless contact between the spacers and the glass is considered, as polytetrafluoroethylene is known for its low friction properties and the normal forces occurring in the simulations are negligible. To avoid rigid body movements, one of the short edges at the symmetry plane of the glass was chosen to have a fixed position.

Tab. 2: Boundary conditions chosen for the simulation study.

Type	Affected component	Property	Value
Symmetry	Glass pane – Absorber inner edge	Symmetrical	-
Contact	Absorber – Connector	Bonded	-
Contact	Primary Sealing – Secondary Sealing	Bonded	-
Contact	Sealings – Connector	Bonded	-
Contact	Sealings – Glass pane	Bonded	-
Contact	Spacer – Absorber	Bonded	-
Contact	Spacer – Glass pane	Frictionless	-
Temperature	Absorber sheets	Constant per simulation	Variable for set of simulations
Temperature	All components	Constant for initial step	20 °C
Convection	Glass pane rear side Connector outer surface (backside)	Constant heat transfer coefficient	3 W/(m²K)
Movement	Glass (edge)	Translation | Rotation	**0 | 0**

The simulation model was used to perform a parametric study regarding various temperature levels. Temperatures, elastoplastic deformation, stresses and strains were then evaluated for the analysis.

2.3 Analysis of Stresses and Strains

The thermo-mechanical simulation was subdivided into a static thermal analysis and a static mechanical analysis. Temperature values were used as an input parameter for the subsequent mechanical simulation. This process was conducted several times to obtain multiple thermo-mechanical results in a temperature range which is representing the load conditions of the solar thermal system. Just like the measured temperatures of the collector array during a whole year, the results were used to derive deformation and strain profiles for the whole year.

For the viscoelastic material (primary sealing), the stress strain relation was computed by the following equation:

$$\boldsymbol{\sigma} = \int_0^t 2G(t-\tau)\frac{d\boldsymbol{e}}{d\tau}d\tau + \boldsymbol{I}\int_0^t K(t-\tau)\frac{d\boldsymbol{\Delta}}{d\tau}d\tau \qquad \text{(eq. 1)}$$

where:

- $\boldsymbol{\sigma}$: Cauchy stress tensor
- t: Current (pseudophyiscal) time
- $G(t)$: shear relaxation kernel function
- τ: past time
- $\boldsymbol{e}$: deviatoric strain tensor
- $\boldsymbol{I}$: unit tensor
- $K(t)$: bulk relaxation kernel function
- $\boldsymbol{\Delta}$: volumetric strain tensor

Since the simulation is a steady-state simulation where the physical time is not representative, the stresses were not evaluated for the thermo-mechanical assessment of the collector primary sealing. The strains in eq. 1, however, are representative and were therefore analyzed for the viscoelastic material (primary sealing).

For the hyperelastic material (secondary sealing), the stress strain relation was computed using the so-called Mooney-Rivlin model (Mooney, 1940; Rivlin, 1948) with two parameters. It is determined by the following equation:

$$\boldsymbol{\sigma} = \frac{1}{J}\boldsymbol{F}\,2\frac{\partial W}{\partial(\boldsymbol{F^T F})}\,\boldsymbol{F^T} \qquad \text{(eq. 2)} \qquad \text{with} \qquad W = c_{10}(\overline{I_1}-3) + c_{01}(\overline{I_2}-3) + \frac{1}{d}(J-1)^2 \qquad \text{and} \qquad J = \det(\boldsymbol{F})$$

where:

$\boldsymbol{F}$:	deformation gradient tensor
W:	strain-energy function per unit undeformed volume
c_{10}:	Mooney-Rivlin material constant
c_{01}:	Mooney-Rivlin material constant
d:	Mooney-Rivlin material constant
$\overline{I_1}, \overline{I_2}, \overline{I_3}$:	principal strains (invariants) of the Cauchy-Green deformation tensor $\boldsymbol{C} = \boldsymbol{F^T F}$

In this case, the stresses are time independent and therefore were evaluated during postprocessing. These results were interpreted further to provide further insights to the durability of the sealings and therefore the collector.

3. Results and Discussion

3.1 Load Analysis

The results of the load analysis were needed both as inputs for the simulation, and to assess the sealing durability after the parametric study. Fig. 8 shows the measured outlet temperature of the collector field during the year 2022. The solar thermal system is active mainly in the months February until November. In the other winter months, the flow temperature may be sufficient to charge storage 2 but undercuts the requirement of 80 °C for the grid. The controllers of the systems are set to maintain a constant feed-in temperature into storage 2 of approximately 90 °C. Despite this target value, a higher peak collector temperature occurred on May 19th 11:20 until 11:35 h with 130°C. Another peak with 128 °C was measured for 5 minutes on May 17th. All remaining peak temperatures in the diagram were below 115 °C. Reasons for this significant overshoot in temperature may be instabilities of the system while controlling the pumps and valves. An entire stagnation of the solar system has not occurred. As long as the solar pump does not fail, stagnation is very unlikely as the thermal power of the solar system is only covering a small share of the total heat demand even in summer operation. Nevertheless, a peak of 130 °C was selected as a maximum temperature for the sealing during normal operation in this investigation.

The annual duration line in Fig. 9 shows the number of hours at which specific temperature levels occurred. This confirms that the number of temperature peaks above 100 °C are present for a limited time of approximately 150 hours per year (1.7 %). For around 575 hours per year (6.6 %), the solar thermal system provides heat in temperature levels that can directly be fed into the grid (> 80 °C) The remaining energy can be fed to storage 2 to increase the grid return temperature. This is particularly the case for 55 °C < T_{out} < 80 °C and yields another 647 hours (7.4 %) where the collector provides solar heat to the system. Consequently, for approximately 7,538 hours in a year (86,1 %) the collector temperature is predominantly affected by the ambient temperature. This analysis of temperature levels for a full-year dataset has therefore shown that short peak temperatures up to 130 °C can occur for a short period of time during a year, and the design temperature for the sealings in normal operation should be considered as approximately 100 °C.

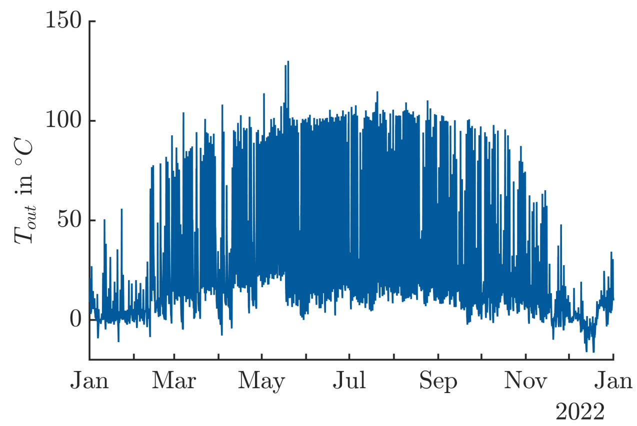

Fig. 8: Measured outlet temperature of the collector field during the year 2022.

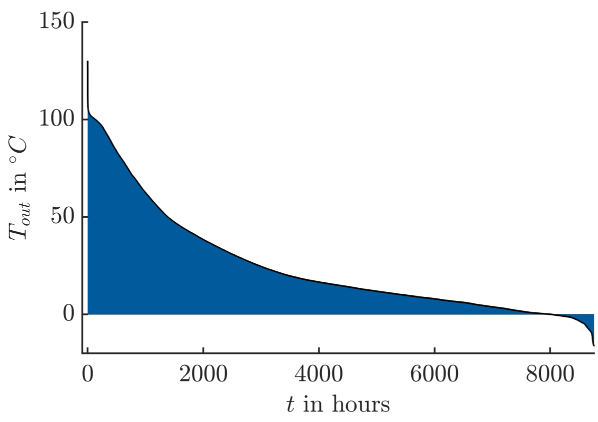

Fig. 9: Annual duration line of collector outlet temperature in the range from 0 to 8760 hours.

In cases where pumps fail or where the solar thermal system is oversized, the heat provided by the collectors cannot be dissipated. This leads to stagnation of the collector. For the analysis, the maximum temperature is calculated using the following equation from the DIN EN ISO 9806 test standard (Deutsches Institut für Normung e. V., 2018).

$$T_{stg} = 1.2\left(T_a + \frac{-a_1+\sqrt{a_1^2+4\eta_0 a_2 G}}{2a_2}\right). \quad \text{(eq. 3)}$$

The stagnation temperature is therefore dependent on the global irradiance G, the ambient temperature T_a, the optical efficiency η_0 of the collector, and its linear (a_1) and quadratic (a_2) thermal loss coefficient. From the latest performance measurements for the respective IGFPCs (Summ et al., 2023) we obtained $\eta_0 = 0.8408$, $a_1 = 3.909$, and $a_2 = 0.01361$. In deviation from the ISO 9806 test standard, we assumed $G = 1225\ \mathrm{Wm^{-2}}$ for considering a more conservative case for regions with very high solar irradiance. Using these parameters for eq. 3, the stagnation temperature of the collector was computed as 236 °C. This maximum temperature was then used to compute the thermo-mechanical reaction of the collector components using the simulation model.

3.2 Thermo-Mechanical Simulation and Analysis of Stresses and Strains

As described in section 2.2, the simulation model first computes the temperature distribution given the thermo-mechanical load conditions described in Tab. 2. The temperature distribution is then used as an input for the mechanical simulation.

3.2.1 Case 1 – Stagnation Temperature

The area of interest is the geometry around the outlet connector. Fig. 10 shows the temperature distribution of the collector in this region. Due to its high thermal conductivity and since its thermal losses inside the collector were neglected, the absorber conducts heat through the connector at high temperatures. The surface of the outlet connector at the back side and the rear surface of the glazing are the only considered heat sinks in the model. As thermal losses at the connector within the collector were neglected, the heat fluxes through the sealings are much more dominant as if these losses were considered and therefore are likely to be overestimated in the model. The glass and its convective heat transfer have a significant cooling effect despite its low thermal conductivity compared to the absorber. As a result, the zone in which the glass experiences significant temperature loads has a size of approximately four times the inner diameter of the sealing.

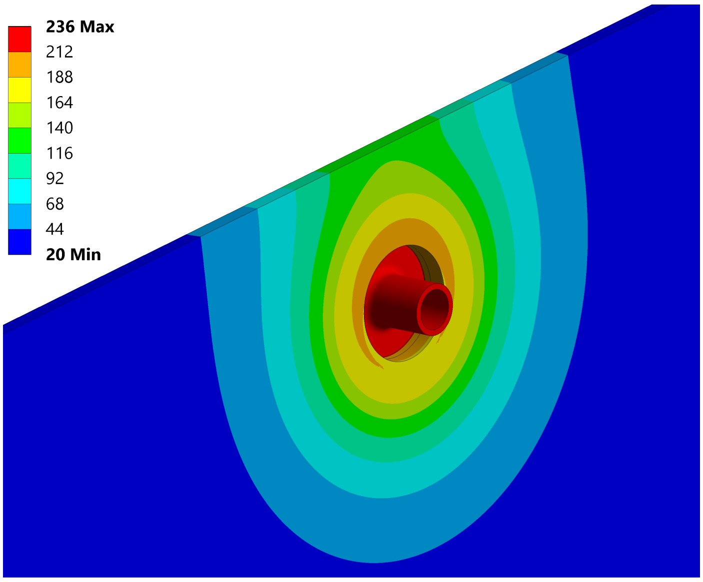

Fig. 10: Temperature distribution (in °C) around the outlet connector in the case of stagnation. The rear side of the collector is shown to indicate the temperature gradients present close to the sealings.

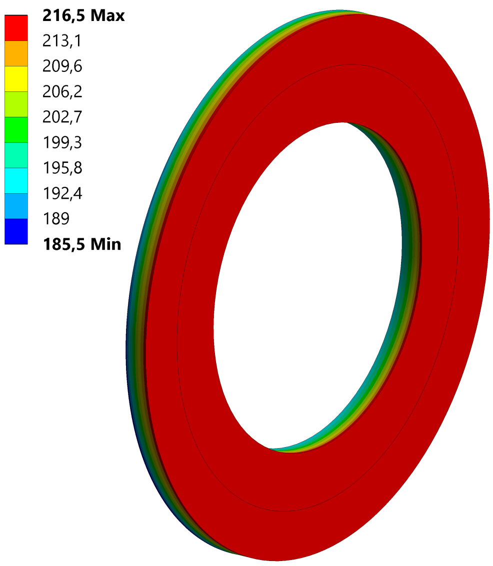

Fig. 11: Temperature distribution (in °C) of the primary and secondary sealings of the outlet connector.

Nevertheless, the convective heat transfer condition at the connector has a cooling effect on the contact area between absorber and sealing. The maximum temperature at this contact surface was observed with 216.5 °C. Fig. 11 shows the temperature distribution within the sealing (undeformed state). On the one hand, the sealings help to reduce thermal bridges from absorber to the ambient by their low thermal conductivity, which is beneficial for the collector efficiency. On the other hand, the sealing temperatures are high consequently. The minimum sealing temperature during stagnation was observed with 185.5 °C and the average temperature with 201.6 °C. As the extreme case of stagnation occurs in the event of a system failure, it is difficult to estimate for how long these temperatures will prevail in the collector. This depends for example on how fast the failure of pumps can be resolved, whether there are clouds during the day or whether there is precipitation. The temperature will also change depending on the solar azimuth and zenith angle. Nevertheless, we expect this extreme temperature may prevail in an unfavorable case for up to 6 to 8 hours on 2 or 3 consecutive days.

The sealing material was designed to withstand constant temperatures up to 130 °C. It can withstand higher temperatures for short-term loads but a definite criterion of failure at temperatures exceeding 130 °C are not given by the manufacturer. At those high temperatures, some ingredients of the sealing may degrade and cause changes to the sealing's thermo-mechanical properties. High-temperature stabilizers will decompose gradually which leads to an increase of the stiffness of the materials. Therefore, the sealings have a reduced ability to compensate for deformations which may lead to leakages. The longer, the material is exposed to excessively high temperatures, the more its flexibility will be reduced and the more likely it is that leakages will occur. The exact time when a leak will occur, is not quantifiable as it depends on a variety of parameters with high degrees of uncertainty such as imperfections during the application of the sealing or unfavorable previous load conditions that are unknown. As a result, there remains a threat for the efficiency of the IGFPCs when it is exposed for too long in the stagnation condition. In contrast, the mechanical stability of the secondary sealing which is required for a reliable operation of the collectors should not be affected by the temperature loads.

The results of the mechanical analysis are shown in Fig. 12. Deformation is magnified by a factor of 6 to visualize the direction in which the components move. As expected, the fixation of the absorber at the two connectors leads to a bending load on the absorber and the sealings. The maximum deformation (displacement) occurred at the absorber edge furthest away from the symmetry plane and was 4.3 mm. This part is not displayed as it has no effect on the sealings. The total deformation of the sealings is significantly smaller.

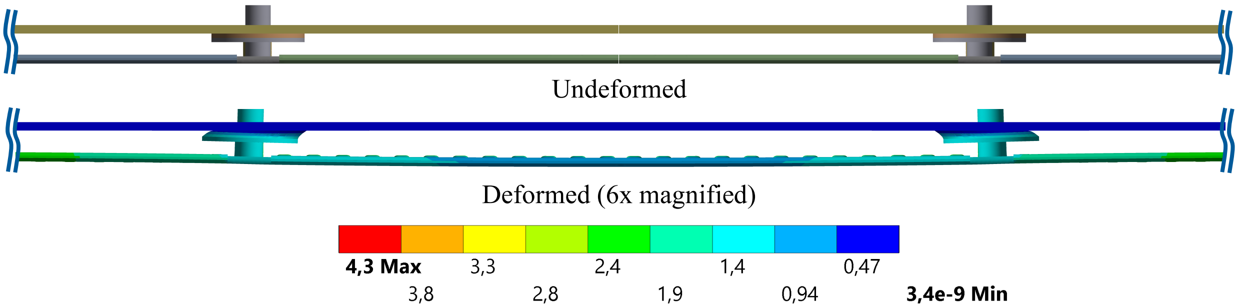

Fig. 12: Comparison of undeformed and deformed (in mm) collector geometry from the top view. The outer left and outer right part of the geometry is not displayed.

In Fig. 13 and Fig. 14 the deformation and mechanical strain of the sealings is shown. For the stagnation case, maximum deformation is 1.4 mm and the corresponding strain 0.501 mm/mm. Using eq. 2, the maximum stress for the secondary sealing was determined as 0.659 MPa. The maximum strains occur at the side facing away from the symmetry plane. For the primary sealing it is 0.439 mm/mm and occurs sparsely in a small region. The average strain is 0.241 mm/mm. For the secondary sealing, the average strain is 0.236 mm/mm and the maximum 0.501 mm/mm.

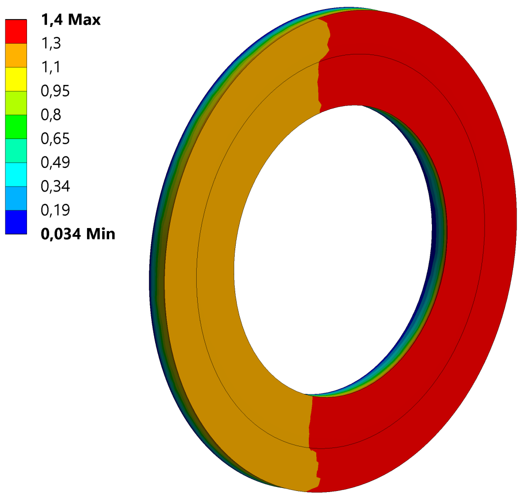

Fig. 13: Deformation (in mm) of the primary and secondary sealings of the inlet/outlet connector.

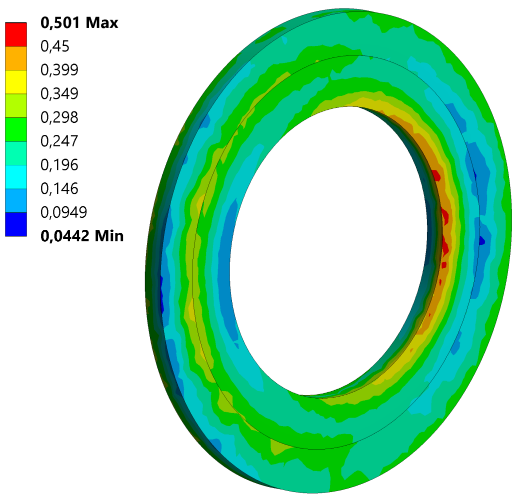

Fig. 14: Strain (in mm/mm) of the primary and secondary sealings of the inlet/outlet connector.

The difference between maximum and average values as well as the sparse presence of peak values within a small part of the sealing indicate, that the sealings may cope with the extreme load conditions for a short period of time.

According to experience from the manufacturer, the maximum strain that the sealings can withstand is approximately 20 % for continuous and 30 % for short term load. Hence, the case of stagnation can be considered as critical (both in terms of temperature and strain) for the lifetime of the sealings. This does affect the efficiency of the modules (gas-tightness) but not its basic functionality (mechanical integrity).

3.2.2 Case 2 – Full-year Load Condition and Parametric Study

To determine the load conditions on the sealings for normal operation during a year, a parametric study was performed for different absorber temperature levels T_{out} ranging from 20 °C to 200 °C. The resulting sealing temperatures, strains, and stress (secondary sealing only) are shown in Tab. 3.

Tab. 3: Simulation results (maximum values) from the parametric study for different absorber temperature levels.

T_{out} °C	T_{pri} °C	T_{sec} °C	ε_{pri} mm/mm	ε_{sec} mm/mm	σ_{sec} MPa
20.0	20.0	20.0	0.004	0.004	0.007
30.0	29.1	29.1	0.017	0.019	0.032
45.0	42.7	42.7	0.045	0.051	0.084
60.0	56.3	56.4	0.075	0.084	0.134
80.0	74.5	74.6	0.119	0.128	0.202
100.0	92.6	92.8	0.162	0.175	0.268
130.0	119.9	120.1	0.227	0.245	0.361
150.0	138.0	138.3	0.269	0.293	0.422
200.0	183.4	183.7	0.370	0.413	0.565

This data was then used to map absorber temperatures to resulting strains in the sealings using linear interpolation (between values listed in Tab. 3) and extrapolation (values below 20 °C). The assembly temperature of the collector was assumed as 20 °C and therefore the stresses and strains that occur for this temperature are numerical noise. For those lower temperatures T_{out}^{-}< 20 °C, the relation $T_{out} = |T_{out}^{-} - 20| + 20$ was used to map temperatures to the strains. In this way, a full-year load curve on the sealings was calculated. These load curves are shown in Fig. 15 and Fig. 16. The figures show that the strains for primary and secondary sealings are well within the limits (0.30 mm/mm for primary and 0.20 for secondary sealing) that the manufacturer of the material defines as the permissible range of application.

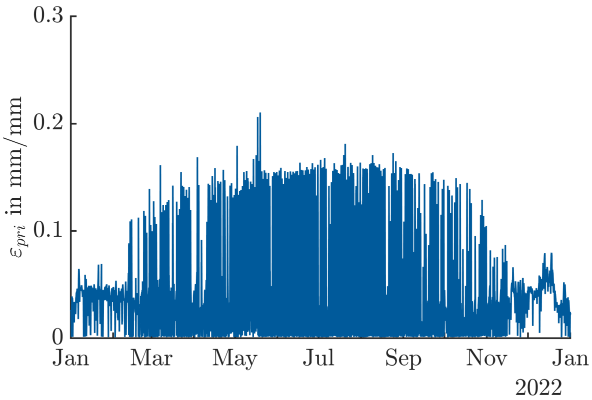

Fig. 15: Time course of the strains (simulated) in the primary sealing for the measured collector temperature loads.

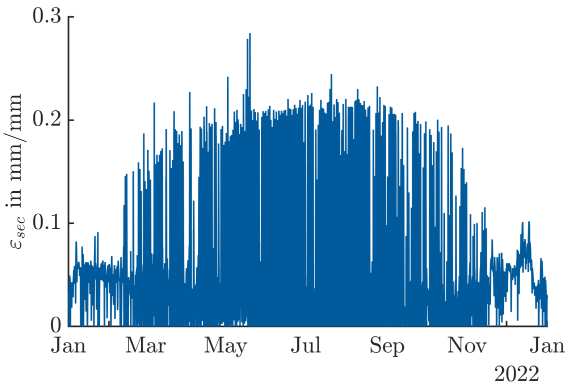

Fig. 16: Time course of the strains (simulated) in the secondary sealing for the measured collector temperature loads.

4. Conclusions

The results of this study have shown, that during stagnation, the thermo-mechanical loads are a critical aspect for the sealings of the insulating glass collector design. This extreme load may affect the efficiency of the modules (gas-tightness) but not its basic functionality (mechanical integrity), which is why the chosen novel design of the collector represents an improvement with respect to collector durability. This advantageous effect was confirmed by results from the loads during normal operation. In that case, the sealing strains and stresses remained within the proposed permissible operating range despite a presumed overestimation of temperatures caused by a series of conservative assumptions. This strongly suggests that the design is durable for its intended use and insulating glass collectors can remain gas-tight for a lifetime of 20 to 25 years. The mechanical results furthermore indicate that absorber deflections are much less critical as compared to previous designs from Riess et al. confirming that the novel design is superior. Finally, we strongly suggest avoiding stagnation for insulating glass collectors by suitable measures such as applying thermochromic coatings to the absorber or emergency generators/batteries with pumps to protect the sealings from overheating. This will help to avoid potential leakages affecting the performance and therefore techno-economic feasibility of the solar thermal system.

Acknowledgments

This work was supported by the Federal Ministry of Economic Affairs and Climate Action of the Federal Republic of Germany within the 7th Energy Research Program under the project “flexLAC” [03ETW015-A].

References

ANSYS, Inc., 2022. ANSYS Mechanical 2022 R2. Software build date: Friday, 27.05.2022 08:55:00, Canonsburg.

Deutsches Institut für Normung, 2010. DIN EN 1991-1-4, Eurocode 1: Einwirkungen auf Tragwerke - Teil 1-4: Allgemeine Einwirkungen - Windlasten. Eurocode 1: Actions on structures - Part 1-4: General actions - Wind actionsloads. Beuth Verlag GmbH, Berlin. Accessed 28 August 2023, 2, 41, 38 Seiten.

Deutsches Institut für Normung, 2023. DIN EN 1991-1-3, Eurocode 1: Einwirkungen auf Tragwerke. Teil 1-3, Allgemeine Einwirkungen - Schneelasten. Eurocode 1: actions on structures. Part 1-3, General actions - snow loads, 1991st ed. ‚Beuth Verlag GmbH, Berlin. Accessed 28 August 2023, 2, 41, 38 Seiten.

Deutsches Institut für Normung e. V., 2018. Solarenergie - Thermische Sonnenkollektoren - Prüfverfahren (ISO 9806:2017); Deutsche Fassung EN ISO 9806:2017. Beuth Verlag GmbH, Berlin.

Giovannetti, F., Kirchner, M., 2015. Performance and Reliability of Insulated Glass Collector Prototypes, in: Proceedings of the EuroSun 2014 Conference, Freiburg, Germany, pp. 355–361. DOI: 10.18086/eurosun.2014.16.07.

Giovannetti, F., Kirchner, M., Kliem, F., Hoeltje, T., 2014. Development of an Insulated Glass Solar Thermal Collector. Energy Procedia 48, 58–66. DOI: 10.1016/j.egypro.2014.02.008.

Leibbrandt, P., Schabbach, T., 2015. Numerical Investigation on Heat Transfer, Fluid Distribution and Solid Stress to a New Type of Solar Flat Plate Collector, in: Proceedings of the EuroSun 2014 Conference, Freiburg, Germany, pp. 1–10. DOI: 10.18086/eurosun.2014.16.13.

Mooney, M., 1940. A Theory of Large Elastic Deformation. Journal of Applied Physics 11 (9), 582–592. DOI: 10.1063/1.1712836.

Riess, H., 2017. Simulation, testing and design of a fully adhesive bonded flat plate solar collector for highly automated production. Ph.D. Thesis. De Montfort University Leicester. https://dora.dmu.ac.uk/bitstream/handle/2086/15041/e-thesis%20submission%20Hermann%20Riess.pdf.

Riess, H., Brandmayr, S., Zörner, W., 2015. A Novel Production Technique for Flat Plate Solar Collectors with a Fully Adhesive Edge Bond, in: Proceedings of the EuroSun 2014 Conference, Freiburg, Germany, pp. 1–9. DOI: 10.18086/eurosun.2014.16.19.

Riess, H., Brandmayr, S., Zörner, W., Greenough, R.M., 2014. Analysis of the Mechanical Behaviour of an All-round Fully Adhesive Supported Absorber. Energy Procedia 48, 201–211. DOI: 10.1016/j.egypro.2014.02.025.

Riess, H., Klärner, M., Zörner, W., Greenough, R., 2016. Thermal Simulation and Efficiency of a Hermetically Sealed Flat Plate Collector with a Fully Adhesive Edge Bond, in: Proceedings of the ISES EuroSun 2016 Conference, Freiburg, Germany, pp. 1100–1113. DOI: 10.18086/eurosun.2016.07.07.

Rivlin, R.S., 1948. Large elastic deformations of isotropic materials IV. further developments of the general theory. Phil. Trans. R. Soc. Lond. A 241 (835), 379–397. DOI: 10.1098/rsta.1948.0024.

Summ, T., Ehrenwirth, M., Trinkl, C., Zörner, W., 2020. Entwicklung eines Großflächenkollektors in Isolierglasbauweise für den Einsatz in Wärmenetzen, in: Online-Symposium Solarthermie und innovative Wärmesysteme. Tagungsunterlagen, pp. 435–448.

Summ, T., Ehrenwirth, M., Trinkl, C., Zörner, W., Pischow, K., Greenough, R., Oyinlola, M., 2023. Effect of argon concentration on thermal efficiency of gas-filled insulating glass flat-plate collectors. Applied Thermal Engineering, 120657. DOI: 10.1016/j.applthermaleng.2023.120657.

Summ, T., Scherer, C., Ehrenwirth, M., Trinkl, C., Zörner, W., 2021. Messtechnische Untersuchung von Kleinmustern eines Isolierglaskollektors anhand von Temperaturbelastungstests, in: Tagungsunterlagen. Online-Symposium Solarthermie und innovative Wärmesysteme. Tagungsunterlagen. Conexio GmbH, Pforzheim, pp. 401–408.